Metadata of the chapter that will be visualized in OnlineFirst

Book Title	Fundamentals of Time-Dependent Density Functional Theory	
Series Title	5304	
Chapter Title	Non-Born–Oppenheimer Dynamics and Conical Intersections	
Copyright Year	2011	
Copyright HolderName	Springer-Verlag Berlin Heidelberg	
Corresponding Author	Family Name	**Casida**
	Particle	
	Given Name	**Mark E.**
	Suffix	
	Division	Département de Chimie Molecularie
	Organization	Laboratoire de Chimie Théorique (DCM, UMR CNRS/UJF 5250), Institut de Chimie Moléculaire de, Grenoble (ICMG, FR2607)
	Address	Grenoble, France
	Email	Mark.Casida@UJF-Grenoble.Fr
Author	Family Name	**Natarajan**
	Particle	
	Given Name	**Bhaarathi**
	Suffix	
	Division	Département de Chimie Molecularie
	Organization	Laboratoire de Chimie Théorique (DCM, UMR CNRS/UJF 5250), Institut de Chimie Moléculaire de, Grenoble (ICMG, FR2607)
	Address	Grenoble, France
	Division	
	Organization	Univ. Joseph Fourier (Grenoble I)
	Address	301 rue de la Chimie, BP 53,, 38041, Grenoble Cedex 9, France
	Division	
	Organization	CEA, INAC, SP2M, L_Sim
	Address	38054, Grenoble Cedex 9, France
	Email	bhaarathi.natarajan@UJF-Grenoble.FR
Author	Family Name	**Deutsch**
	Particle	
	Given Name	**Thierry**
	Suffix	
	Division	
	Organization	CEA, INAC, SP2M, L_Sim
	Address	38054, Grenoble Cedex 9, France
	Email	thierry.deutsch@cea.fr

Abstract

The area of excited-state dynamics is receiving increasing attention for a number of reasons. First the importance of photochemical processes in basic energy sciences, improved theoretical methods and the associated theoretical understanding of photochemical processes. Then there is the advent of femtosecond (and now attosecond) spectroscopy Femtosecond spectroscopy allowing access to more detailed experimental

information about photochemical processes. Since photophysical and chemical processes are more complex than thermal (i.e., ground state) processes, simulations quickly become expensive and even unmanageable as the model system becomes increasingly realistic. With its combination of simplicity and yet relatively good accuracy, TDDFT has been finding an increasingly important role to play in this rapidly developing field. After reviewing some basic ideas from photophysics and photochemistry, this chapter will cover some of the strengths and weaknesses of TDDFT for modeling photoprocesses.

Chapter 14
Non-Born–Oppenheimer Dynamics and Conical Intersections

Mark E. Casida, Bhaarathi Natarajan and Thierry Deutsch

14.1 Introduction

The area of excited-state dynamics is receiving increasing attention for a number of reasons. First the importance of photochemical processes in basic energy sciences, improved theoretical methods and the associated theoretical understanding of photochemical processes. Then there is the advent of femtosecond (and now attosecond) spectroscopy allowing access to more detailed experimental information about photochemical processes. Since photophysical and chemical processes are more complex than thermal (i.e., ground state) processes, simulations quickly become expensive and even unmanageable as the model system becomes increasingly realistic. With its combination of simplicity and yet relatively good accuracy, TDDFT has been finding an increasingly important role to play in this rapidly developing field. After reviewing some basic ideas from photophysics and photochemistry, this chapter will

M. E. Casida (✉) · B. Natarajan
Département de Chimie Moleculaire,
Laboratoire de Chimie Théorique (DCM, UMR CNRS/UJF 5250),
Institut de Chimie Moléculaire de, Grenoble (ICMG, FR2607),
Grenoble, France
e-mail: Mark.Casida@UJF-Grenoble.Fr

B. Natarajan
e-mail: bhaarathi.natarajan@UJF-Grenoble.FR

B. Natarajan · M. E. Casida
Univ. Joseph Fourier (Grenoble I),
301 rue de la Chimie, BP 53,
38041 Grenoble Cedex 9, France

T. Deutsch
CEA, INAC, SP2M, L_Sim, 38054 Grenoble Cedex 9, France
e-mail: thierry.deutsch@cea.fr

M. A. L. Marques et al. (eds.), *Fundamentals of Time-Dependent Density Functional Theory*, Lecture Notes in Physics 837, DOI: 10.1007/978-3-642-23518-4_14,

270015_1_En_14_Chapter ☑ TYPESET ☐ DISK ☐ LE ☑ CP Disp.:10/8/2011 Pages: 21 Layout: T1-Standard

cover some of the strengths and weaknesses of TDDFT for modeling photoprocesses. The emphasis will be on going beyond the Born–Oppenheimer approximation.

There are distinct differences between how solid-state physicists and chemical physicists view photoprocesses. We believe that some of this is due to fundamental differences in the underlying phenomena being studied but that much is due to the use of different approximations and the associated language. Ultimately anyone who wants to work at the nanointerface between molecules and solids must come to terms with these differences, but that is not our objective here. Instead we will adapt the point of view of a chemical physicist (or physical chemist)—see, e.g. (Michl and Bonačić-Koutecký 1990).

The usual way to think about molecular dynamics is in terms of the potential energy surfaces that come out of the Born–Oppenheimer separation. In thermal processes, vibrations are associated with small motions around potential energy surface minima. Chemical reactions are usually described as going over passes (transition states) on these hypersurfaces as the system moves from one valley (reactants) to another (products). Photoprocesses are much more complicated (see Fig. 14.1). Traditionally they include not only process that begin by absorption of a photon, but also any process involving electronically excited states, such as chemiluminescence (e.g., in fireflies and glow worms) where the initial excitation energy is provided by a chemical reaction. The Franck–Condon approximation tells us that the initial absorption of a photon will take us from one vibronic state to another without much change of molecular geometry, thus defining a Franck–Condon region on the excited-state potential energy surfaces. The molecule can return to the ground state by emitting a photon of the initial wavelength or, depending upon vibronic coupling and perturbations from surrounding molecules, the molecule may undergo radiationless relaxation to a lower energy excited state before emitting or it may even decay all the way to the ground state without emitting. If emission takes place from a long-lived excited state of the same spin as the ground state, then we speak of fluorescence. If emission takes place from an excited-state with a different spin due to intersystem crossing, then we speak of phosphorescence. If it is unsure whether the emission is fluorescence or phosphorescence, then we just say the molecule luminesces. Because of the large variety of de-excitation processes, excited molecules usually return too quickly to their ground state for the molecular geometry to change much. We then speak of a photophysical process because no chemical reaction has taken place. Thus fluorescence is usually described as an excited molecule relaxing slightly to a nearby minimum on the excited-state potential energy surface where it is momentarily trapped before it emits to the ground state. It follows that the photon emitted during fluorescence is Stokes shifted to a lower energy than that of the photon initially absorbed.

Photochemical reactions occur when the excited molecule decays to a new minimum on the ground state surface, leading to a new chemical species (product). This may have positive value as a way for synthesizing new mole-cules or negative value because of photodegradation of materials or because of photochemically-induced cancers. Either way the photochemical reaction must occur quickly enough that it can compete with other decay processes. Photochemical reactions almost

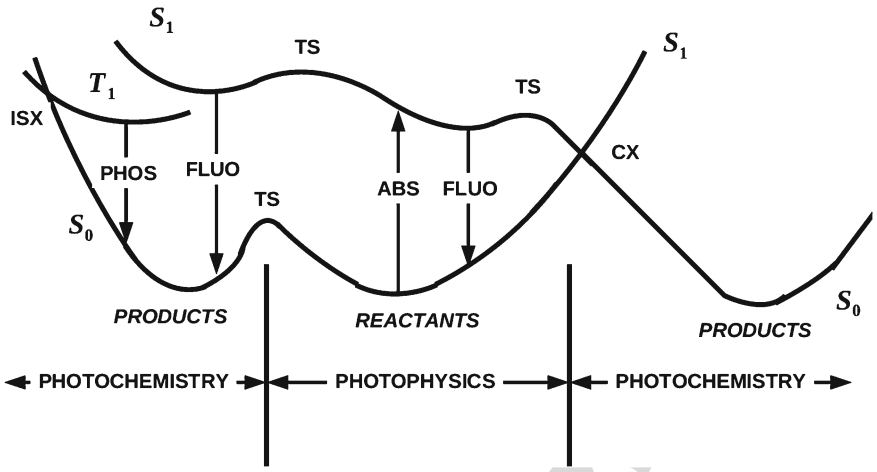

Fig. 14.1 Schematic representation of potential energy surfaces for photophysical and photochemical processes: S_0 ground singlet state; S_1 lowest excited singlet state; T_1 lowest triplet state; *ABS* absorption; *FLUO* fluorescence; *PHOS* phosphorescence; *ISX* intersystem crossing; *CX* conical intersection; *TS* transition state.

always occur via photochemical funnels where excited-state and ground-state surfaces come together, either almost touching (avoided crossing) or crossing (conical intersection.) These funnels play a role in photochemical reactions similar to transition states for thermal reactions. However it must be kept in mind that these funnels may be far from the Franck–Condon region on the excited-state potential energy surface, either because there is an easy energetically-"downhill" process or because, unless the absorption wavelength can be carefully tuned to a known vertical excitation energy, the system will typically arrive in an electronically-excited state with excess dynamical energy which can be used to move from one excited-state potential energy surface valley over a transition state to funnels in another basin of the excited-state potential energy surface. While conical intersections are forbidden in diatomic molecules, they are now believed to be omnipresent in the photochemistry of polyatomic molecules. Traditional simple models involve symmetry constraints which correspond to a potential energy surface cut, typically revealing an avoided crossing rather than the nearby conical intersection corresponding to a less symmetric geometry. A particularly striking example is provided by experimental and theoretical evidence that the fundamental photochemical reaction involved in vision passes through a conical intersection (Polli et al. 2010). For these reasons, modern photochemical modeling often involves some type of dynamics and, when this is not possible, at least focuses on finding conical intersections that can explain the reaction.

While a single-reference electronic structure method may be adequate for describing photophysical processes, the usual standard for describing photochemical processes is a multireference electronic structure method such as the complete active space self-consistent field (CASSCF) method. [See (Helgaker et al. 2000) for a review

of modern quantum chemical methods]. This is because the first approximation to the wave function along a reaction pathway is as a linear combination of the wave functions of the initial reactants and the final products. Since CASSCF is both computationally heavy and requires a high-level of user intervention, a simpler method such as TDDFT would be very much welcome. Early work in TDDFT in quantum chemistry foresaw increasing applications of TDDFT in photochemical modeling. For example, avoided crossings between cross-sections of excited-state potential energy surfaces may be described with TDDFT because of the multireference-like nature of TDDFT excited states (Casida 1998a, b). However great attention must also be paid to problems arising from the use of approximate functionals (Casida 2002). In particular, the TDDFT Tamm-Dancoff approximation (TDA) (Hirata 1999) was found to give improved shapes of excited-state potential energy surfaces (Casida 2000; Cordova et al. 2007), albeit at the price of losing oscillator strength sum rules. A major advance towards serious investigations of TDDFT for describing photoprocesses came with the implementation of analytical derivatives for photochemical excited states in many electronic structure programs [see Chap. 16 and (Van Caillie and Amos 1999, 2000; Furche and Ahlrichs 2002a; Hutter 2003; Rappoport and Furche 2005; Doltsinis and Kosov 2005; Scalmani et al. 2006)]. This made it possible to relax excited-state geometries and to calculate Stokes shifts within the framework of TDDFT. In fact, TDDFT has become a standard part of the photochemical modeler's toolbox. It is typically used for calculating absorption spectra and exploring excited-state potential energy surfaces around the Franck–Condon region. TDDFT also serves as a rapid way to gain the chemical information needed to carry out subsequent CASSCF calculations. [See, e.g., (Diau et al. 2001a, b, 2002; Sølling et al. 2002; Diau and Zewail 2003) for some combined femtosecond spectroscopy/theoretical studies of photochemical reactions which make good use of TDDFT.] It would be nice to be able to use a single method to model entire photochemical processes. The advent of mixed TDDFT/classical surface-hopping Tully-type dynamics (Tapavicza et al. 2007; Werner et al. 2008; Tapavicza et al. 2008; Tavernelli et al. 2009a, c; Barbatti et al. 2010) is giving us a way to extend the power of TDDFT to the exploration of increasingly complicated photochemical processes.

The rest of this chapter is organized as follows: The next section reviews non-Born–Oppenheimer phenomena from a wave-function point of view, with an emphasis on mixed quantum/classical dynamics. This sets the stage for our discussion of TDDFT for non-Born–Oppenheimer dynamics and conical intersections in Sect. 14.3. We sum up in Sect. 14.4.

14.2 Wave-Function Theory

Most likely anyone who has made it this far into this chapter has seen the Born–Oppenheimer approximation at least once, if not many times. However, it is relatively rare to find good discussions that go beyond the Born–Oppenheimer approximation (Doltsinis and Marx 2002; Cederbaum 2004). This section tries to do just this from a

wave-function point of view, in preparation for a discussion of TDDFT approaches to the same problems in the following section. We first begin by reviewing (again!) the Born–Oppenheimer approximation, but this time with the point of view of identifying the missing terms. We then discuss mixed quantum/classical approximations, and end with a discussion of the pathway method and ways to find and characterize conical intersections. (Mixed quantum/quantum and quantum/semiclassical methods are also interesting, but have been judged beyond the scope of this chapter.) We shall use Hartree atomic units ($\hbar = m_e = e = 1$) throughout and adapt the convention in this section that electronic states are labeled by small Latin letters, while nuclear degrees of freedom are labeled by capital Latin letters.

14.2.1 Born–Oppenheimer Approximation and Beyond

As is well-known, the Born–Oppenheimer approximation relies on a separation of time scales: Since electrons are so much lighter and so move so much faster than nuclei, the electrons may be thought of as moving in the field of nuclei which are "clamped" in place and the nuclei move in a field which is determined by the mean field of the electrons. The Born–Oppenheimer approximation provides a precise mathematical formulation of this physical picture. Our interest here is in where the Born–Oppenheimer approximation breaks down and what terms are needed to describe this breakdown.

Consider a molecule composed of M nuclei and N electrons. Denote the nuclear coordinates by $\bar{\boldsymbol{R}} = (\boldsymbol{R}_1, \boldsymbol{R}_2, \ldots, \boldsymbol{R}_M)$ and electronic coordinates by $\bar{\boldsymbol{r}} = (\boldsymbol{r}_1, \boldsymbol{r}_2, \ldots, \boldsymbol{r}_N)$. The full Hamiltonian, $\hat{H}(\bar{\boldsymbol{R}}, \bar{\boldsymbol{r}}) = \hat{T}_\mathrm{n}(\bar{\boldsymbol{R}}) + \hat{H}_\mathrm{e}(\bar{\boldsymbol{r}}; \bar{\boldsymbol{R}}) + V_\mathrm{nn}(\bar{\boldsymbol{R}})$, is the sum of an electronic Hamiltonian, $\hat{H}_\mathrm{e}(\bar{\boldsymbol{r}}; \bar{\boldsymbol{R}}) = \hat{T}_\mathrm{e}(\bar{\boldsymbol{r}}) + V_\mathrm{en}(\bar{\boldsymbol{r}}; \bar{\boldsymbol{R}}) + V_\mathrm{ee}(\bar{\boldsymbol{r}})$, with its electronic kinetic energy, $\hat{T}_\mathrm{e}$, electron-nuclear attraction, V_en, and electron–electron repulsion, V_ee, with the missing nuclear terms—namely the nuclear kinetic energy, $\hat{T}_\mathrm{n}$, and the nuclear–nuclear repulsion, V_nn. Solving the time-dependent Schrödinger equation,

$$\hat{H}(\bar{\boldsymbol{R}}, \bar{\boldsymbol{r}})\widetilde{\Psi}(\bar{\boldsymbol{R}}, \bar{\boldsymbol{x}}, t) = \mathrm{i}\frac{\mathrm{d}}{\mathrm{d}t}\widetilde{\Psi}(\bar{\boldsymbol{R}}, \bar{\boldsymbol{x}}, t), \tag{14.1}$$

is a formidable $(N + M)$-body problem. ($\bar{\boldsymbol{x}}$ denotes inclusion of electron spin. We have decided to omit nuclear spin for simplicity. Note, however, that explicit inclusion of nuclear spin can sometimes be important—for example, the properties of *ortho*- and *para*-hydrogen.) That is why the Born–Oppenheimer expansion (which is not yet the Born–Oppenheimer approximation!),

$$\Phi(\bar{\boldsymbol{R}}, \bar{\boldsymbol{x}}, t) = \sum_j \Psi_j(\bar{\boldsymbol{x}}; \bar{\boldsymbol{R}})\chi_j(\bar{\boldsymbol{R}}, t), \tag{14.2}$$

is used, where the electronic wave functions are solutions of the time-independent electronic problem in the field of clamped nuclei,

$$\hat{H}_{\rm e}(\bar{\boldsymbol{r}};\bar{\boldsymbol{R}})\Psi_j(\bar{\boldsymbol{x}};\bar{\boldsymbol{R}}) = E_j^{\rm e}(\bar{\boldsymbol{R}})\Psi_j(\bar{\boldsymbol{x}};\bar{\boldsymbol{R}}). \tag{14.3}$$

Inserting the Born–Oppenheimer expansion (Eq. 14.2) into the full Schrödinger equation (Eq. 14.1), left multiplying by $\Psi_i^*(\bar{\boldsymbol{x}};\bar{\boldsymbol{R}})$, and integrating over $\bar{\boldsymbol{x}}$ gives the time-dependent Schrödinger equation for the nuclear degrees of freedom,

$$\left[\hat{T}_{\rm n}(\bar{\boldsymbol{R}}) + V_i(\bar{\boldsymbol{R}})\right]\chi_i(\bar{\boldsymbol{R}},t) + \sum_j \hat{V}_{i,j}(\bar{\boldsymbol{R}})\chi_j(\bar{\boldsymbol{R}},t) = \mathrm{i}\frac{\partial}{\partial t}\chi_i(\bar{\boldsymbol{R}},t). \tag{14.4}$$

Here, $V_i(\bar{\boldsymbol{R}}) = E_i^{\rm e}(\bar{\boldsymbol{R}}) + V_{\rm nn}(\bar{\boldsymbol{R}})$, is the *adiabatic* potential energy surface for the ith electronic state. [Notice that this is a different use of the term "adiabatic" than in the TDDFT "adiabatic approximation" for the exchange-correlation (xc) functional.] The remaining part, $\hat{V}_{i,j}(\bar{\boldsymbol{R}})$, is the hopping term which couples the Ith and Jth potential energy surfaces together. It should be kept in mind that the Born–Oppenheimer expansion (Eq. 14.2) is exact and hence so is Eq. 14.4. As is well known, the Born–Oppenheimer approximation neglects the hopping terms,

$$\left[\hat{T}_{\rm n}(\bar{\boldsymbol{R}}) + V_i(\bar{\boldsymbol{R}})\right]\chi_i(\bar{\boldsymbol{R}},t) = \mathrm{i}\frac{\partial}{\partial t}\chi_i(\bar{\boldsymbol{R}},t). \tag{14.5}$$

We, on the other hand, are interested in precisely the terms neglected by the Born–Oppenheimer approximation. The hopping term is given by

$$\hat{V}_{i,j}(\bar{\boldsymbol{R}})\chi_j(\bar{\boldsymbol{R}},t) = -\sum_I \frac{1}{2m_I}\left[G_{i,j}^{(I)}(\bar{\boldsymbol{R}}) + 2\boldsymbol{F}_{i,j}^{(I)}(\bar{\boldsymbol{R}})\cdot\nabla_I\right]\chi_j(\bar{\boldsymbol{R}},t), \tag{14.6}$$

where,

$$\begin{aligned} G_{i,j}^{(I)}(\bar{\boldsymbol{R}}) &= \int \mathrm{d}^3\bar{x}_1\cdots\int \mathrm{d}^3\bar{x}_N\,\Psi_i^*(\bar{\boldsymbol{x}};\bar{\boldsymbol{R}})\left[\nabla_I^2\Psi_j(\bar{\boldsymbol{x}};\bar{\boldsymbol{R}})\right] \\ &= \langle i|\nabla_I^2|j\rangle, \end{aligned} \tag{14.7}$$

is the scalar coupling matrix and,

$$\begin{aligned} \boldsymbol{F}_{i,j}^{(I)}(\bar{\boldsymbol{R}}) &= \int \mathrm{d}^3\bar{x}_1\cdots\int \mathrm{d}^3\bar{x}_N\,\Psi_i^*(\bar{\boldsymbol{x}};\bar{\boldsymbol{R}})\left[\nabla_I\Psi_j(\bar{\boldsymbol{x}};\bar{\boldsymbol{R}})\right] \\ &= \langle i|\nabla_I|j\rangle, \end{aligned} \tag{14.8}$$

is the derivative coupling matrix (Cederbaum 2004). Note that the derivative coupling matrix is also often denoted $\boldsymbol{d}_{i,j}^I$ and called the nonadiabatic coupling vector (Doltsinis and Marx 2002). Here we have introduced a compact notation for some complicated objects: Both the scalar and derivative coupling matrices are simultaneously a function of the nuclear coordinates, a matrix in the electronic degrees of freedom, and a vector in the nuclear degrees of freedom, and a matrix in the electronic degrees of freedom. However the derivative coupling matrix is also a vector in the three spatial coordinates of the Ith nucleus.

Interestingly the scalar coupling matrix and derivative coupling matrix are not independent objects. Rather, making use of the resolution of the identity for the electronic states, it is straightforward to show that,

$$\sum_k \left(\delta_{i,k}\nabla_I + \boldsymbol{F}^{(I)}_{i,k}(\bar{\boldsymbol{R}})\right)\cdot\left(\delta_{k,j} + \nabla_I \boldsymbol{F}^{(I)}_{k,j}(\bar{\boldsymbol{R}})\right) = \nabla_I^2 + G^{(I)}_{i,j}(\bar{\boldsymbol{R}}) + 2\boldsymbol{F}^{(I)}_{i,j}(\bar{\boldsymbol{R}})\cdot\nabla_I. \tag{14.9}$$

We may then rewrite the time-dependent nuclear equation (14.4) as,

$$-\left\{\sum_I \frac{1}{2m_I}\left[\sum_k \left(\delta_{i,j}\nabla_I + \boldsymbol{F}^{(I)}_{i,k}(\bar{\boldsymbol{R}})\right)\cdot\left(\delta_{k,j}\nabla_I + \boldsymbol{F}^{(I)}_{k,j}(\bar{\boldsymbol{R}})\right)\right]\right\}\chi_j(\bar{\boldsymbol{R}},t) + V_i(\bar{\boldsymbol{R}})\chi_i(\bar{\boldsymbol{R}},t) = \mathrm{i}\frac{\partial}{\partial t}\chi_j(\bar{\boldsymbol{R}},t), \tag{14.10}$$

which is known as the group Born–Oppenheimer equation (Cederbaum 2004). Evidently this is an equation which can be solved within a truncated manifold of a few electronic states in order to find fully quantum mechanical solutions beyond the Born–Oppenheimer approximation.

More importantly for present purposes is that Eq. 14.10 brings out the importance of the derivative coupling matrix. The derivative coupling matrix can be rewritten as,

$$\boldsymbol{F}^{(I)}_{i,j}(\bar{\boldsymbol{R}}) = \frac{\langle i|\left[\nabla_I \hat{H}_e(\bar{\boldsymbol{R}})\right]|j\rangle - \delta_{i,j}\nabla_I E^e_i(\bar{\boldsymbol{R}})}{E^e_j(\bar{\boldsymbol{R}}) - E^e_i(\bar{\boldsymbol{R}})}. \tag{14.11}$$

Since this equation is basically a force-like term, divided by an energy difference, we see that we can neglect coupling between adiabatic potential energy surfaces when (i) the force on the nuclei is sufficiently small (i.e., the nuclei are not moving too quickly) and (ii) when the energy difference between potential energy surfaces is sufficiently large.

These conditions often break down in funnel regions of photochemical reactions. There is then a tendency to follow diabatic surfaces, which may be defined rigorously by a unitary transformation of electronic states (when it exists) to a new representation satisfying the condition, $\boldsymbol{F}^{(I)}_{i,j}(\bar{\boldsymbol{R}}) \approx 0$. The advantage of the diabatic representation (when it exists, which is not always the case) is that it eliminates the off-diagonal elements of the derivative coupling matrix in the group Born–Oppenheimer equation (Eq. 14.10), hence eliminating the need to describe surface hopping. At a more intuitive level, the character of electronic states tends to be preserved along diabatic surfaces because

$$\left\langle i|\frac{\mathrm{d}j}{\mathrm{d}t}\right\rangle = \dot{\boldsymbol{R}}\cdot\langle i|\nabla j\rangle = \dot{\boldsymbol{R}}\cdot\boldsymbol{F}_{i,j} \approx 0 \tag{14.12}$$

in this representation. For this reason, it is usual to trace diabatic surfaces informally in funnel regions by analyzing electronic state character, rather than seeking to minimize

the nonadiabatic coupling vector. Avoided crossings of adiabatic surfaces are then described as due to configuration mixing of electronic configurations belonging to different diabatic surfaces.

14.2.2 Mixed Quantum/Classical Dynamics

Solving the fully quantum-mechanical dynamics problem of coupled electrons and nuclei is a challenge for small molecules and intractable for larger molecules. Instead it is usual to use mixed quantum/classical methods in which the nuclei are described by Newtonian classical mechanics while the electrons are described by quantum mechanics. Dividing any quantum system into two parts and then approximating one using classical mechanics is the subject of on-going research (Kapral 2006). In general, no rigorous derivation is possible and wave-function phase information (e.g., the Berry phase) is lost which may be important in some instances. Nevertheless mixed quantum/classical approximations are intuitive: Most nuclei (except perhaps hydrogen) are heavy enough that tunneling and other quantum mechanical effects are minor, so that classical dynamics is often an *a priori* reasonable first approximation. Of course, rather than thinking of a single classical trajectory for the nuclear degree of freedom, we must expect to think in terms of ensembles (or "swarms") of trajectories which are built to incorporate either finite temperature effects or to try to represent quantum mechanical probability distributions or both. The purpose of this subsection is to introduce some common mixed quantum/classical methods.

The most elementary mixed quantum/classical approximation is Ehrenfest dynamics. According to Ehrenfest's (1927) theorem Newton's equations are satisfied for mean values in quantum systems, $\mathrm{d}\langle\hat{\boldsymbol{r}}\rangle/\mathrm{d}t = \langle\hat{\boldsymbol{p}}\rangle/m$ and $\mathrm{d}\langle\hat{\boldsymbol{p}}\rangle/\mathrm{d}t = -\langle\nabla V\rangle$. Identifying the position of the nuclei with their mean value, we can then write an equation, $m_I\ddot{\bar{\boldsymbol{R}}}_I(t) = -\nabla_I V(\bar{\boldsymbol{R}}(t))$, whose physical interpretation is that the nuclei are moving in the mean field of the electrons. Here

$$V(\bar{\boldsymbol{R}}(t)) = \langle\Psi(\bar{\boldsymbol{R}},t)|\hat{H}_\mathrm{e}(\bar{\boldsymbol{R}}(t))|\Psi(\bar{\boldsymbol{R}},t)\rangle + V_\mathrm{nn}(\bar{\boldsymbol{R}}(t)), \tag{14.13}$$

where the electronic wave function is found by solving the time-dependent equation,

$$\hat{H}_\mathrm{e}(\bar{\boldsymbol{x}},\bar{\boldsymbol{R}}(t))\Psi(\bar{\boldsymbol{x}};\bar{\boldsymbol{R}},t) = \mathrm{i}\frac{\partial}{\partial t}\Psi(\bar{\boldsymbol{x}};\bar{\boldsymbol{R}},t). \tag{14.14}$$

While Ehrenfest dynamics has been widely and often successfully applied, it suffers from some important drawbacks. The first drawback is that the nuclei always move on average potential energy surfaces, rather than adiabatic or diabatic surfaces, even when far from funnel regions where the nuclei would be expected to move on the surface of a single electronic state. While this is serious enough, since it suggests errors in calculating branching ratios (i.e., relative yields of different products in a photoreaction), a more serious drawback is a loss of microscopic reversibility.

That is, the temporal variation of the mean potential energy surface depends upon past history and can easily be different for forward and reverse processes.

A very much improved scheme is the fewest switches method of Tully (1990) (Hammes-Schiffer and Tully 1994). Here the nuclei move on well-defined adiabatic potential energy surfaces,

$$m_I \ddot{\bar{\boldsymbol{R}}}_I(t) = -\nabla_I V_i(\bar{\boldsymbol{R}}(t)), \tag{14.15}$$

and the electrons move in the field of the moving nuclei,

$$\hat{H}_{\mathrm{e}}(\bar{\boldsymbol{r}}; \bar{\boldsymbol{R}}(t))\Psi(\bar{\boldsymbol{x}}, t) = \mathrm{i}\frac{\mathrm{d}}{\mathrm{d}t}\Psi(\bar{\boldsymbol{x}}, t). \tag{14.16}$$

To determine the probability that a classical trajectory describing nuclear motion hops from one electronic potential energy surface to another, we expand

$$\Psi(\bar{\boldsymbol{x}}, t) = \sum_m \Psi_m(\bar{\boldsymbol{x}}; \bar{\boldsymbol{R}}(t))C_m(t), \tag{14.17}$$

in solutions of the time-independent Schrödinger equation,

$$\hat{H}(\bar{\boldsymbol{r}}; \bar{\boldsymbol{R}}(t))\Psi_m(\bar{\boldsymbol{x}}; \bar{\boldsymbol{R}}(t)) = E_m(\bar{\boldsymbol{R}}(t))\Psi_m(\bar{\boldsymbol{x}}; \bar{\boldsymbol{R}}(t)). \tag{14.18}$$

The probability of finding the system on surface m is then given by, $P_m(t) = |C_m(t)|^2$. The coefficients may be obtained in a dynamics calculation by integrating the first-order equation,

$$\dot{C}_m(t) = -\mathrm{i}E_m(t)C_m(t) - \sum_n \left\langle m|\frac{\mathrm{d}n}{\mathrm{d}t}\right\rangle C_n(t). \tag{14.19}$$

A not unimportant detail is that the nonadiabatic coupling elements need not be calculated explicitly, but instead can be calculated using the finite difference formula,

$$\langle m(t + \Delta t/2)|\dot{n}(t + \Delta t/2)\rangle = \frac{\langle m(t)|n(t + \Delta t)\rangle - \langle m(t + \Delta t)|n(t)\rangle}{2\Delta t}. \tag{14.20}$$

In practice, it is also important to minimize the number of surface hops or switches in order to keep the cost of the dynamics calculation manageable. [Tully also suggests (p. 1066 of Ref. (Tully 1990)) that too rapid switching would lead to trajectories behaving incorrectly *as if* they were on an average potential energy surface.] Tully accomplished this by introducing his fewest-switches algorithm which is a type of Monte Carlo procedure designed to correctly populate the different potential energy surfaces with a minimum of surface hopping. Briefly, the probability of jumping from surface m to surface n in the interval $(t, t + \Delta t)$ is given by $g_{m\to n}(t, \Delta t) = \dot{P}_{m,n}(t)\Delta t / P_{m,m}(t)$ where $P_{m,n}(t) = C_m(t)C_n^*(t)$. A random number ξ is generated with uniform probability on the interval (0,1) and compared with $g_{m\to n}(t, \Delta t)$. The

transition $m \rightarrow n$ occurs only if $P_n^{(m-1)} < \xi < P_n^{(m)}$ where $P_n^{(m)} = \sum_{l=1,m} P_{n,l}$ is the sum of the transition probabilities for the first m states. Additional details of the algorithm, beyond the scope of this chapter, involve readjustment of nuclear kinetic energies and the fineness of the numerical integration grid for the electronic part of the calculation with respect to that of the grid for the nuclear degrees of freedom.

It is occasionally useful to have a simpler theory for calculating the probability of potential energy surface hops which depends only on the potential energy surfaces and not on the wave functions. Such a theory was suggested by Landau (1932) and Zener (1932) (see also Wittig 2005). Their work predates the modern appreciation of the importance of conical intersections and so focused on surface hopping at avoided crossings. The Landau–Zener model assumes that surface hopping occurs only on the surface where the two diabatic surfaces cross that give rise to the avoided crossing where the surface hopping occurs. After some linearizations and an asymptotic limit, it is possible to arrive at a very simple final formula,

$$P = \exp\left[-\frac{\pi^2 \Delta E_{\text{adia}}^2}{h(\mathrm{d}|\Delta E_{\text{dia}}|/\mathrm{d}t)}\right], \tag{14.21}$$

for the probability of hopping between two potential energy surfaces. This formula is to be applied at the point of closest approach of the two potential energy surfaces where the energy difference is ΔE_{adia}. However $\mathrm{d}|\Delta E_{\text{dia}}|/\mathrm{d}t$ is evaluated as the maximum of the rate of change of the *adiabatic* energy difference as the avoided crossing is approached. While not intended to be applied to conical intersections, it is still applicable in photodynamics calculations in the sense that trajectories rarely go exactly through a conical intersection.

14.2.3 Pathway Method

Dynamics calculations provide a swarm of reaction trajectories. The "pathway method" provides an alternative when dynamics calculations are too expensive or a simplified picture is otherwise desired, say, for interpretational reasons. The pathway method consists of mapping out minimum energy pathways between the initial Franck–Condon points obtained by vertical excitations and excited-state minima or conical intersections. Although analogous to the usual way of finding thermal reaction paths, it is less likely to be a realistic representation of true photoprocesses except in the limit of threshold excitation energies since excess energy is often enough to open up alternative pathways over excited-state transition states. While the necessary ingredients for the photochemical pathway method are similar to those for thermal reactions, conical intersections are a new feature which is quite different from a thermal transition state. This section provides a brief review for finding and characterizing conical intersections.

The notion of a conical intersection arises from a relatively simple argument (Yarkony 2001). The potential energy surface of a molecule with f internal degrees of

freedom is an f-dimensional hypersurface in an $(f+1)$-dimensional space (the extra dimension is the energy axis). If two potential energy surfaces simply cross "without seeing each other", then the crossing space is characterized by the constraint

$$E_i(\bar{\boldsymbol{R}}) = E_j(\bar{\boldsymbol{R}}), \tag{14.22}$$

making the crossing space $(f-1)$-dimensional. However in quantum mechanics, we also have the additional constraint,

$$H_{i,j}(\bar{\boldsymbol{R}}) = 0. \tag{14.23}$$

This makes the crossing space $(f-2)$-dimensional. This means that there will be two independent directions in hyperspace in which the two potential energy surfaces will separate. These two directions define a branching plane. Within the 3-dimensional space defined by the energy and the branching plane, the conical intersection appears to be a double cone (see Fig. 14.6), the point of which represents an entire $(f-1)$-dimensional space. Of course, $f=1$ for a diatomic and no conical intersection is possible. This is the origin of the well-known avoided crossing rule for diatomics. Here we are interested in larger molecules where the low dimensionality of the branching space in comparison with the dimensionality of the parent hyperspace can make the conical intersection hard to locate and characterize.

In the pathway method, the system simply goes energetically downhill until two potential energy surfaces have the same energy (Eq. 14.22). The resultant intersection space must be analyzed and the branching plane extracted so that the surface crossing region can be properly visualized and interpreted. In order to do so, let us recall a result from elementary calculus. Imagine a trajectory, $\bar{\boldsymbol{R}}(\tau)$, depending upon some parameter τ within the conical intersection surface. Then $\nabla\mathcal{C}(\bar{\boldsymbol{R}})$ must be perpendicular to the conical intersection for any constraint function $\mathcal{C}(\bar{\boldsymbol{R}}) = 0$ because,

$$0 = \frac{\mathrm{d}\mathcal{C}(\bar{\boldsymbol{R}}(\tau))}{\mathrm{d}\tau} = \nabla\mathcal{C}(\bar{\boldsymbol{R}}) \cdot \frac{\mathrm{d}\bar{\boldsymbol{R}}}{\mathrm{d}\tau}. \tag{14.24}$$

and we can always choose $\mathrm{d}\bar{\boldsymbol{R}}/\mathrm{d}\tau \neq 0$. Taking the gradient of Eq. 14.23 defines the derivative coupling vector, $\boldsymbol{f}_{i,j} = \nabla H_{i,j}(\bar{\boldsymbol{R}})$, while taking the gradient of Eq. 14.22 defines the gradient difference vector, $\boldsymbol{g}_{i,j} = \nabla E_i(\bar{\boldsymbol{R}}) - \nabla E_j(\bar{\boldsymbol{R}})$. Together the derivative coupling vector and gradient difference vector are referred to as the branching vectors which characterize the branching plane. [Note that the derivative coupling vector is essentially the numerator of the derivative coupling matrix expression given in Eq. 14.11. This confusion of nomenclature is unfortunate but present in the literature.]

The condition that $\mathrm{d}\bar{\boldsymbol{R}}/\mathrm{d}\tau$ be perpendicular to the branching plane provides a constraint for use in the exploration of the conical intersection hyperspace when seeking the minimum energy conical intersection or the first-order saddle point

in conical intersection. In particular, there has been considerable effort devoted to the problem of developing efficient algorithms for finding minimum energy points within the conical intersection space (Koga and Morokuma 1985; Atchity et al. 1991; Ragazos et al. 1992; Yarkony 1996; Domcke and Stock 1997; Izzo and Klessinger 2000). Furthermore, an automated systematic exploration method for finding minimum energy conical intersections has very recently developed (Maeda et al. 2009). First-order saddle points and the corresponding minimum energy pathways both within the conical intersection hypersurface may be useful reference points when mapping out a surface, and an optimization method was developed for such high-energy points within the conical intersection hypersurface (Sicilia et al. 2008). Some of the minimum energy conical intersection optimizers use the branching plane conditions explicitly to keep the degeneracy of the two adiabatic states during optimizations (Manaa and Yarkony 1993; Bearpark et al. 1994; Anglada and Bofill 1997), making explicit use of both the derivative coupling vector and gradient difference vector at every step. Most well-estabilished optimization algorithms assume smoothness of the function to be optimized. Since the potential energy surface necessarily has a discontinuous first derivative in the vicinity of a conical intersection, the above-mentioned algorithms for finding minimum energy conical intersections have required access to the gradient difference vector and derivative coupling vectors. The gradient difference vector can easily be obtained from analytical gradients, if available, or by numerical energy differentiation if analytical gradients are not yet available. However ways for finding the derivative coupling vector are not yet available for all methods since implementation of an analytical derivative method is often regarded as a prerequisite (Ciminelli et al. 2004; Maeda et al. 2010). Some approaches make use of a penalty function to get around the need to calculate the derivative coupling vector and these have proven very useful for finding minimum energy conical intersection regions without the need for the derivative coupling vector (Levine et al. 2008). This is especially important for methods such as renormalized coupled-cluster theories and TDDFT or free-energy methods for which the electronic wave function is not completely defined, considerably complicating the problem of how to calculate derivative coupling vector matrix elements. However, convergence of penalty function methods is in general slower than methods which make explicit use of the branching plane constraints, especially if tight optimization of the energy difference, $(E_i - E_j)$, is desired (Keal et al. 2007).

14.3 TDDFT

The last section discussed the basic theory of non-Born–Oppenheimer dynamics and conical intersections from a wave-function point of view. We now wish to see to what extent we can replace wave-function theory with what we hope will be a simpler DFT approach. As usual in DFT, we seek both the guiding light of formal rigor and pragmatic approximations that work. We will take a more or less historical approach to

presenting this material. In this section, upper case Latin indices designate electronic states, while lower case Latin indices designate orbitals.

One of the early objectives of TDDFT was to allow simulations of the behavior of atoms and clusters in intense laser fields, well beyond the linear-response regime and too complex to be handled by comparable wave-function methods. The closely related topic of ion-cluster collisions was studied early on using TDDFT in a very simplified form (Yabana et al. 1998). The Ehrenfest method was the method of choice for TDDFT simulations coupling electronic and nuclear degrees of freedom in this area. The gradient of the potential (14.13) is calculated with the help of the Hellmann-Feynman theorem as,

$$\nabla_I V(\bar{\boldsymbol{R}}(t)) = \langle \Psi(\bar{\boldsymbol{R}}, t) | \nabla_I \hat{H}_{\mathrm{e}}(\bar{\boldsymbol{R}}(t)) | \Psi(\bar{\boldsymbol{R}}, t) \rangle + \nabla_I V_{\mathrm{nn}}(\bar{\boldsymbol{R}}(t)). \tag{14.25}$$

Note that the first integral on the right hand side only involves the (time-dependent) charge density—at least in the usual TDDFT adiabatic approximation. Among the notable work done with this approximation is early studies of the dynamics of sodium clusters in intense laser fields (Calvayrac et al. 1998), the development of the time-dependent electron localization function (Burnus et al. 2005), and (more recently) the study of electron-ion dynamics in molecules under intense laser pulses [see Chap. 18 and (Kawashita et al. 2009)]. Besides limitations associated with the TDDFT adiabatic approximation, the TDDFT Ehrenfest method suffers from the same intrinsic problems as its wave-function sibling—namely that it is implicitly based on an average potential energy surface and so does not provide state-specific information, and also suffers from problems with microscopic irreversibility.

To our knowledge, the first DFT dynamics on a well-defined excited-state potential energy surface was not based upon TDDFT but rather on the older multiplet sum method of Ziegler et al. (1977) (Daul 1994). This was the work of restricted open-shell Kohn-Sham (ROKS) formalism of Irmgard Frank et al. (1998) who carried out Car-Parinello dynamics for the open-shell singlet excited state $^1(i, a)$ using the multiplet sum method energy expression,

$$E_s = 2E\left[\Phi_{i\uparrow}^{a\uparrow}\right] - E\left[\Phi_{i\downarrow}^{a\uparrow}\right], \tag{14.26}$$

where $\Phi_{i\sigma}^{a\tau}$ is the Kohn-Sham determinant with the $i\sigma$ spin-orbital replaced with the $a\tau$ spin-orbital. Such a formalism suffers from all the formal difficulties of the multiplet sum method, namely that it is just a first-order estimate of the energy using a symmetry-motivated zero-order guess for the excited-state wave function and assumes that DFT works best for states which are well-described by single determinants. Nevertheless appropriate use of the multiplet sum method can yield results similar to TDDFT. A recent application of this method is to the study of the mechanism of the electrocyclic ring opening of diphenyloxirane (Friedrichs and Frank 2009).

The implementation of TDDFT excited-state derivatives in a wide variety of programs not only means that excited-state geometry optimizations may be implemented, allowing the calculation of the Stokes shift between absorption and fluorescence spectra, but that the pathway method can be implemented to search for

conical intersections in TDDFT. Unless nonadiabatic coupling matrix elements can be calculated within TDDFT (*vide infra*), then a penalty method should be employed as described in the previous section under the pathway method. This has been done by Levine et al. (2006) using conventional TDDFT and by Minezawa and Gordon (2009) using spin-flip TDDFT. We will come back to these calculations later in this section.

The most recent approach to DFT dynamics on a well-defined excited-state potential energy surface is Tully-type dynamics (Tully 1990; Hammes-Schiffer and Tully 1994; Tully 1998a) applied within a mixed TDDFT/classical trajectory surface-hopping approach. Surface-hopping probabilities can be calculated from potential energy surfaces alone within the Landau–Zener method (Eq. 14.21), however a strict application of Tully's method requires nonadiabatic coupling matrix elements as input. Thus a key problem to be addressed is how to calculate nonadiabatic coupling matrix elements within TDDFT. Initial work by Craig, Duncan, and Prezhdo used a simple approximation which neglected the xc-kernel (Craig et al. 2005). A further approximation, commented on by Maitra (2006b), has been made by Craig and co-workers (Craig et al. 2005; Habenicht et al. 2006) who treated the electronic states as determinants of Kohn-Sham orbitals which are propagated according to the time-dependent Kohn-Sham equation. This means that neither the excitation energies nor the associated forces could be considered to be accurate.

The first complete mixed TDDFT/classical trajectory surface-hopping photodynamics method was proposed and implemented by Tapavicza, Tavernelli, and Röthlisberger (Tapavicza et al. 2007) in a development version of the CPMD code. It was proposed that the nonadiabatic coupling matrix elements be evaluated within Casida's *ansatz* (Casida 1995) which was originally intended to aid with the problem of assigning excited states by considering a specific functional form for an approximate excited-state wave function. Note that numerical integration of Eq. 14.19 to estimate the coefficients, $C_m(t)$, for the true system of interacting electrons also involves making assumptions about the initial interacting excited state. Casida's *ansatz* is a more logical choice for this than is a simple single determinant of Kohn-Sham orbitals. For the TDA, the Casida *ansatz* takes the familiar form, $\Psi_I = \sum_{ia\sigma} \Phi_{i\sigma}^{a\sigma} X_{ia\sigma}$.

In fact, matrix elements between ground and excited states may be calculated exactly in a Casida-like formalism because of the response theory nature of Eq. 14.11 (Chernyak Mukamel 2000a, Hu 2007b, Send 2010). Test results show reasonable accuracy for nonadiabatic coupling matrix elements as long as conical intersections are not approached too closely (Baer 2002; Hu et al. 2007b; Tavernelli 2009c; Tavernelli et al. 2009a; Send and Furche 2010). One likely reason for this is the divergence of Eq. 14.11 when $E_I = E_J$. Hu and Sugino attempted to further improve the accuracy of nonadiabatic coupling matrix elements by using average excitation energies (Hu Sugino 2007a). The problem of calculating nonadiabatic coupling matrix elements between two excited states is an open problem in TDDFT, though the ability to calculate excited-state densities (Furche and Ahlrichs 2002a) suggests that such matrix elements could be calculated from double response theory using Eq. 14.11. The idea is that adding a second time-dependent electric field *in*

addition to the first perturbation which allows the extraction of excited-state densities, should allow the extraction of the excited-state absorption spectrum using linear response theory in much the same way that this is presently done for the ground state. To our knowledge, this has never yet been done. But were it to be done, the extension to the derivative coupling matrix through Eq. 14.11 should be trivial.

Soon after the implementation of mixed TDDFT/classical trajectory surface-hopping photodynamics in CPMD, a very similar method was implemented in TURBOMOL and applied (Werner et al. 2008, Mirić et al. 2008, Barbatti et al. 2010). A version of TURBOMOL capable of doing mixed TDDFT/classical trajectory surface-hopping photodynamics using analytic nonadiabatic coupling matrix elements (see Chap. 16) has recently appeared (Send and Furche 2010) and has been used to study the photochemistry of vitamin-D (Tapavicza 2010). Time-dependent density-functional tight-binding may be regarded as the next step in a multiscale approach to the photodynamics of larger systems. From this point of view, it is interesting to note that mixed TDDFT-tight binding/classical trajectory surface-hopping photodynamics is also a reality (Mitrić et al. 2009). Given the increasingly wide-spread nature of implementations of mixed TDDFT/classical trajectory surface-hopping photodynamics, we can only expect the method to be increasingly available to and used by the global community of computational chemists.

Before going further, let us illustrate the state-of-the-art for TDDFT when applied to non-Born–Oppenheimer dynamics and conical intersections. We will take the example of the photochemical ring opening of oxirane (structure I in Fig. 14.2). While this is not the "sexy application" modeling of some biochemical photoprocess, the photochemistry of oxiranes is not unimportant in synthetic photochemistry and, above all, this is a molecule where it was felt that TDDFT "ought to work" (Cordova et al. 2007). A first study showed that a main obstacle to photodynamics is the presence of triplet and near singlet instabilities which lead to highly underestimated and even imaginary excitation energies as funnel regions are approached. This is illustrated in Fig. 14.3 for C_{2v} ring opening. While the real photochemical process involves asymmetric CO ring-opening rather than the symmetric C_{2v} CC ring-opening, results for the symmetric pathway have the advantage of being easier to analyze. The figure shows that applying the TDA strongly attenuates the instability problem, putting most curves in the right energy range. Perhaps the best way to understand this is to realize that, whereas time-dependent Hartree–Fock (TDHF), is a nonvariational method and hence allows variational collapse of excited states, TDA TDHF is the same as configuration interaction singles (CIS) which is variational. There is however still a cusp in the ground state curve as the ground state configuration changes from σ^2 to $(\sigma^*)^2$. According to a traditional wave-function picture, these two states, which are each double excitations relative to each other should be included in configuration mixing in order to obtain a proper description of the ground state potential energy surface in the funnel region [see Chap. 8 and (Cordova et al. 2007; Huix-Rotllant et al. 2010)].

Figure 14.4 shows an example of mixed TDA TDPBE/classical trajectory surface-hopping calculations for the photochemical ring-opening of oxirane with the initial photoexcitation prepared in the $^1(n, 3p_z)$ state. Part (b) of the figure clearly shows

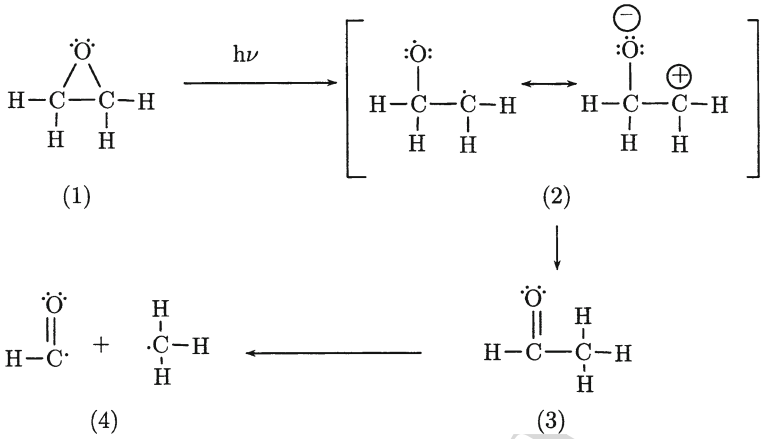

Fig. 14.2 Mechanism proposed by Gomer and Noyes in 1950 for the photochemical ring opening of oxirane. Reprinted with permission from (Tapavicza et al. 2008). Copyright 2008, American Institute of Physics

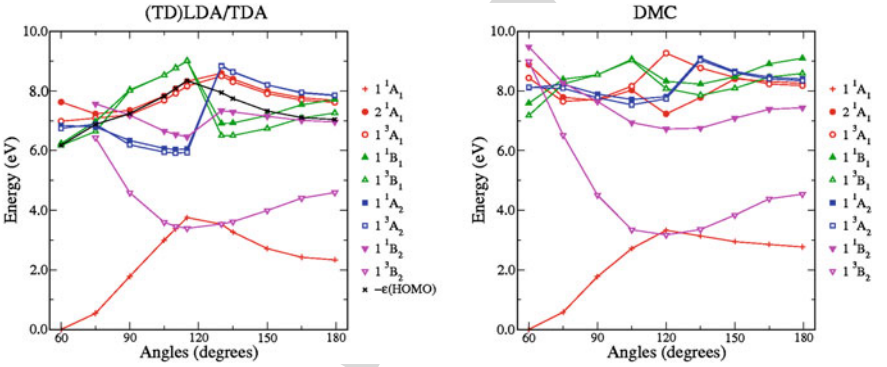

Fig. 14.3 Comparison of TDA TDLDA and diffusion Monte Carlo curves for C_{2v} ring opening of oxirane. Reprinted with permission from Cordova et al. (2007). Copyright 2007, American Institute of Physics

that more than one potential energy surface is populated after about 10 fs. The Landau–Zener process is typical of the dominant physical process which involves an excitation from the HOMO nonbonding lone pair on the oxygen initially to a $3p_z$ Rydberg orbital. As the reaction proceeds, the ring opens and the target Rydberg orbital rapidly changes character to become a CO σ^* antibonding orbital (Fig. 14.5). Actual calculations were run on a swarm of 30 trajectories, confirming the mechanism previously proposed Gomer–Noyes mechanism (Gomer and Noyes 1950) (Fig. 14.2), but also confirming other experimental by-products and giving unprecedented state-specific reaction details such as the orbital description briefly described above.

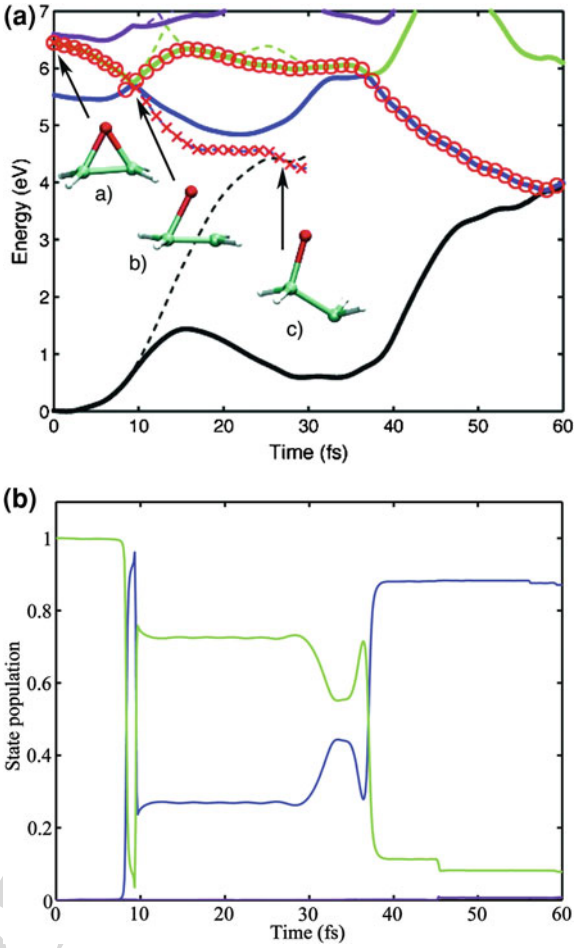

Fig. 14.4 **a** Cut of potential energy surfaces along reaction path of a Landau–Zener (*dashed line*) and a fewest-switches (*solid line*) trajectory (*black*, S_0; *blue*, S_1; *green*, S_2; *magenta*, S_3). Both trajectories were started by excitation into the $^1(n, 3p_z)$ state, with the same geometry and same initial nuclear velocities. The running states of the Landau–Zener and the fewest-switches trajectory are indicated by the *red crosses* and *circles*, respectively. The geometries of the Landau–Zener trajectory are shown at time *a* 0, *b* 10, and *c* 30 fs. **b** State populations (*black*, S_0; *blue*, S_1; *green*, S_2; *magenta*, S_3) as a function of the fewest-switches trajectory in (**a**). Reprinted with permission from Tapavicza et al. (2008). Copyright 2008, American Institute of Physics

The oxirane photochemical ring-opening passes through a conical intersection, providing a concrete example of a conical intersection to study with TDDFT. We now return to the study by Levine, Ko, Quenneville, and Martinez of conical intersections using conventional TDDFT (Levine and Piris 2006) who noted that strict conical intersections are forbidden by the TDDFT adiabatic approximation for the simple reason that there is no coupling matrix element (Eq. 14.23) to zero out between the ground and excited states. Figure 14.6 shows a CASSCF conical intersection close to the oxirane photochemical funnel. Also shown are the TDA TDDFT surfaces calculated with the same CASSCF branching coordinates. Interestingly the CASSCF and TDDFT conical intersections look remarkably similar. However closer examination shows that the TDDFT "conical intersection" is actually two *intersecting* cones rather than a true conical intersection, confirming the observation of Levine *et al*. This was analyzed in detail in Tapavicza et al. (2008) where it was concluded that the problem

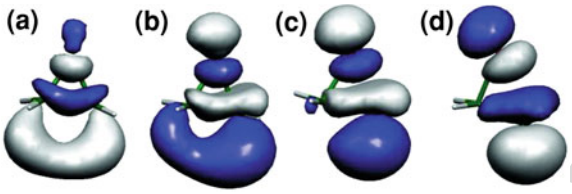

Fig. 14.5 Change of character of the active state along the reactive Landau–Zener trajectory, shown in Fig. 14.1. Snapshots were taken at times **a** 2.6, **b** 7.4, **c** 12.2, and **d** 19.4 fs. For **a** and **b**, the running state is characterized by a transition from the highest occupied molecular orbital (HOMO) to the lowest unoccupied molecular orbital (LUMO) plus one (LUMO + 1), while for **c** and **d** it is characterized by a HOMO–LUMO transition due to orbital crossing. Note that the HOMO remains the same oxygen nonbonding orbital throughout the simulation. Reprinted with permission from Tapavicza et al. (2008). Copyright 2008, American Institute of Physics

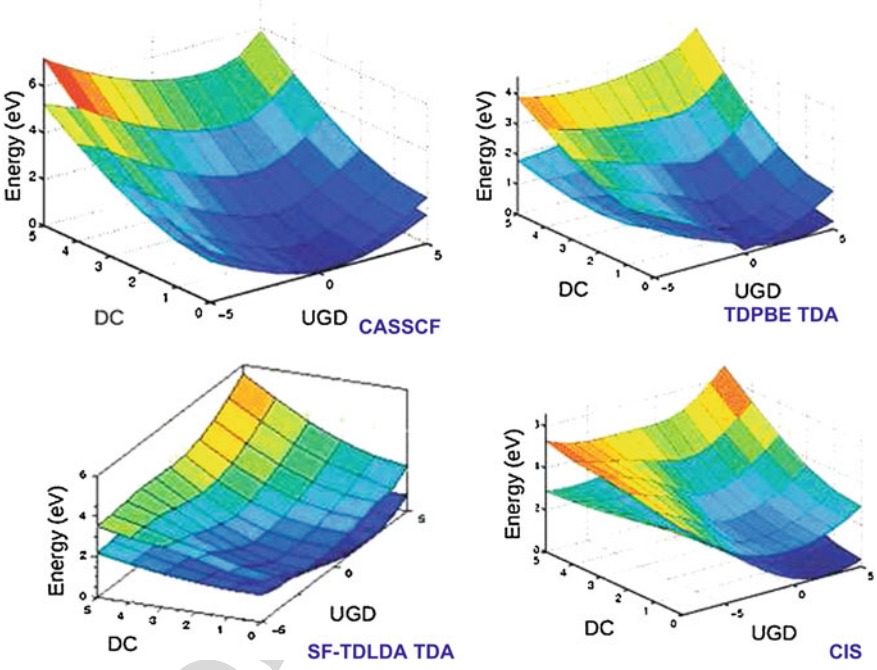

Fig. 14.6 Comparison of the S_0 and S_1 potential energy surfaces calculated using different methods for the CASSCF branching coordinate space. Reproduced from Huix-Rotllant et al. (2010) by permission of the PCCP Owner Societies

is that we are encountering effective noninteracting *v*-representability. True noninteracting *v*-representability means that there is no noninteracting system whose ground state gives the ground state density of the interacting system. This only means that there is some excited state of the noninteracting system with integer occupation number which gives the ground state density of the interacting system. What we

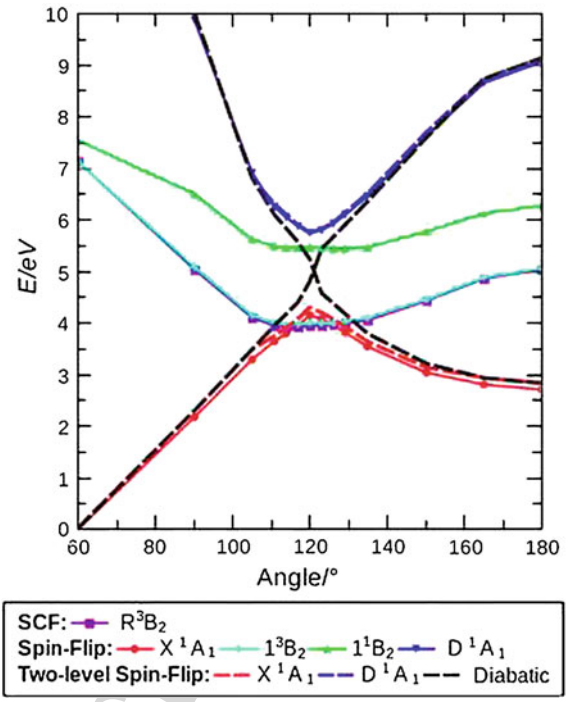

Fig. 14.7 C_{2v} potential energy curves: full calculation (*solid lines*), two-orbital model (*dashed lines*). Reproduced from Huix-Rotllant et al. (2010) by permission of the PCCP Owner Societies

call effective noninteracting *v*-representability is when the LUMO falls below the HOMO (or, in the language of solid-state physics, there is a "hole below the Fermi level"). This is exactly what frequently happens in the funnel region.

Spin-flip (SF) TDDFT (Slipchenko and Krylov 2003; Shao et al. 2003; Wang and Ziegler 2004) offers one way to circumvent some of the problems of effective noninteracting *v*-representability in funnel regions. This is because we can start from the lowest triplet state which has fewer effective noninteracting *v*-representability problems and then use SFs to obtain both the ground state and a doubly-excited state (see Chap. 8). Analytic derivatives are now available for some types of SF-TDDFT (Seth et al. 2010). Figure 14.7 shows that SF-TDDFT works fairly well for treating the avoided crossing in the C_{2v} ring-opening pathway of oxirane. Minezawa and Gordon also used SF-TDDFT to locate a conical intersection in ethylene (Minezawa and Gordon 2009). However Huix-Rotllant, Natarajan, Ipatov, Wawire, Deutsch, and Casida found that, although SF-TDDFT does give a true conical intersection in the photochemical ring opening of oxirane, the funnel is significantly shifted from the position of the CASSCF conical intersection (Huix-Rotllant 2010). The reason is that the key funnel region involves an active space of over two orbitals which is too large to be described accurately by SF-TDDFT.

There are other ways to try to build two- and higher-excitation character into a DFT treatment of excited states. Let us mention here only multireference configu-

ration interaction (MRCI)/DFT (Grimme and Waletzke 1999), constrained density functional theory-configuration interaction (CDFT-CI) (Wu et al. 2007), and mixed TDDFT/many-body theory methods based upon the Bethe-Salpeter equation (Romaniello 2009) or the related polarization propagator approach (Casida 2005; Huix-Rotllant and Casida 2011a) or the simpler dressed TDDFT (Maitra et al. 2004; Cave et al. 2004; Gritsenko and Baerends 2009, Mazur and WÃlodarczyk 2009, Mazur 2010, Huix-Rotllant et al. 2011b) approach.

All of these may have the potential to improve the DFT-based description of funnel regions in photochemical reactions. Here however we must be aware that we may be in the process of building a theory which is less automatic and requires the high amount of user intervention typical of present day CASSCF calculations. This is certainly the case with CDFT-CI which has already achieved some success in describing conical intersections (Kaduk and Van Voorhis 2010).

14.4 Perspectives

Perhaps the essence of dynamics can be captured in a simple sentence: "You should know from whence you are coming and to where you are going." Of course this rather deterministic statement must be interpreted differently in classical and quantum mechanics. Here however we would like to think about its meaning in terms of the development of DFT for applications in photoprocesses. Theoretical developments in this area have been remarkable in recent years, opening up the possibility for a more detailed understanding of femtosecond (and now also attosecond) spectroscopy. In this chapter we have tried to discuss the past, the present, and a bit of the future.

The past treated here has been the vast area of static investigation and dynamic simulations of photophysical and photochemical processes. We have first described more traditional wave-function techniques. We have also mentioned and made appropriate references to important work on early DFT work involving Ehrenfest TDDFT and restricted open-shell Kohn-Sham DFT dynamics. Our emphasis has been on photochemical processes involving several potential energy surfaces, partly because of our own personal experiences, but also because photo*chemical* processes start out as photo*physical* processes in the Franck–Condon region and then rapidly become more complicated to handle.

The present-day status of DFT photodynamics is perhaps best represented by the recent availability of mixed TDDFT and TDDFTB/classical surface-hopping dynamics codes as well as serious efforts to investigate and improve the quality of the TDDFT description of photochemical funnel regions. First applications have already shown the utility of this theory and we feel sure that other applications will follow as programs are made broadly available to computational scientists. Finally

we have ended the last section with some speculations about the future concerning the need for explicit double- and higher-excitations to correctly describe funnel regions.

As expected, we could not treat everything of relevance to the chapter title. Roi Baer's recent work indicating that Berry phase information is somehow included in the ground-state charge density is most intriguing (Baer 2010a). Also on-going work on multicomponent DFT capable of treating electrons and nuclei on more or less the same footing (Kreibich and Gross 2001a, Kreibich et al. 2008) would seem to open up new possibililties for developing useful non-Born–Oppenheimer approximations within a DFT framework. We are sure that still other potentially relevant work has been unfortunately omitted either because of space limitations or for other reasons.

Do we know where this field is going? Certainly non-Born–Oppenheimer photodynamics using some form of DFT is currently a hot and rapidly evolving area. Exactly what lies in store may not yet be clear, but what we do know is that we are going to have fun getting there!

Book: 270015_1_En
Chapter: 14

Springer
the language of science

Author Query Form

Please ensure you fill out your response to the queries raised below and return this form along with your corrections

Dear Author

During the process of typesetting your chapter, the following queries have arisen. Please check your typeset proof carefully against the queries listed below and mark the necessary changes either directly on the proof/online grid or in the 'Author's response' area provided below

Query	Details required	Author's response
1.	Please provide high-resolution artwork for Fig. 14.6.	
2.	Please check the affiliation of all authors.	
3.	References "Tapavicza (2010) and Mazur (2010)" are not found in Book back matter. Please check.	

MARKED PROOF

Please correct and return this set

Please use the proof correction marks shown below for all alterations and corrections. If you wish to return your proof by fax you should ensure that all amendments are written clearly in dark ink and are made well within the page margins.

Instruction to printer	*Textual mark*	*Marginal mark*
Leave unchanged	··· under matter to remain	
Insert in text the matter indicated in the margin		New matter followed by or
Delete	through single character, rule or underline or through all characters to be deleted	or
Substitute character or substitute part of one or more word(s)	through letter or through characters	new character or new characters
Change to italics	under matter to be changed	
Change to capitals	under matter to be changed	
Change to small capitals	under matter to be changed	
Change to bold type	under matter to be changed	
Change to bold italic	under matter to be changed	
Change to lower case	Encircle matter to be changed	
Change italic to upright type	(As above)	
Change bold to non-bold type	(As above)	
Insert 'superior' character	through character or where required	or under character e.g. or
Insert 'inferior' character	(As above)	over character e.g.
Insert full stop	(As above)	
Insert comma	(As above)	
Insert single quotation marks	(As above)	or and/or or
Insert double quotation marks	(As above)	or and/or or
Insert hyphen	(As above)	
Start new paragraph		
No new paragraph		
Transpose		
Close up	linking characters	
Insert or substitute space between characters or words	through character or where required	
Reduce space between characters or words	between characters or words affected	